Exact on-event expressions for discrete potential systems

Marcus N. Bannerman[1,2,a)] and Leo Lue[1,3,b)]
[1]*School of Chemical Engineering and Analytical Science, The University of Manchester, Oxford Road, Manchester M13 9PL, United Kingdom*
[2]*Institute for Multiscale Simulation, Universität Erlangen-Nürnberg, 91052 Erlangen, Germany*
[3]*Department of Chemical and Process Engineering, University of Strathclyde, James Weir Building, 75 Montrose Street, Glasgow G1 1XJ, United Kingdom*

(Received 11 July 2010; accepted 14 August 2010; published online 24 September 2010)

The properties of systems composed of atoms interacting though discrete potentials are dictated by a series of events which occur between pairs of atoms. There are only four basic event types for pairwise discrete potentials and the square-well/shoulder systems studied here exhibit them all. Closed analytical expressions are derived for the on-event kinetic energy distribution functions for an atom, which are distinct from the Maxwell–Boltzmann distribution function. Exact expressions are derived that directly relate the pressure and temperature of equilibrium discrete potential systems to the rates of each type of event. The pressure can be determined from knowledge of only the rate of core and bounce events. The temperature is given by the ratio of the number of bounce events to the number of disassociation/association events. All these expressions are validated with event-driven molecular dynamics simulations and agree with the data within the statistical precision of the simulations. © *2010 American Institute of Physics*. [doi:10.1063/1.3486567]

I. INTRODUCTION

The interaction energy between two square-well/shoulder atoms, one of type α and the other of type α', separated by a distance r is given by

$$u(r) = \begin{cases} \infty & \text{for } 0 < r < \sigma_{\alpha\alpha'} \\ \pm\varepsilon_{\alpha\alpha'} & \text{for } \sigma_{\alpha\alpha'} < r < \lambda_{\alpha\alpha'}\sigma_{\alpha\alpha'} \\ 0 & \text{for } \lambda_{\alpha\alpha'}\sigma_{\alpha\alpha'} < r \end{cases}, \quad (1)$$

where $\sigma_{\alpha\alpha'}$ is the exclusion diameter of the pair of atoms, $\varepsilon_{\alpha\alpha'}$ is a positive value that characterizes the strength of the interaction between the atoms, and $\lambda_{\alpha\alpha'}$ characterizes the range of the interaction (see Fig. 1). Square-shoulder (+) and square-well systems (−) differ only in the sign of the $\pm\varepsilon_{\alpha\alpha'}$ term. The square-well potential is particularly interesting as it captures the essential physics of the interactions between real atoms: short-ranged excluded volume repulsions and intermediate ranged attractions.

Due to their fundamental importance and the relative ease of their simulation, the properties of square-well and square-shoulder systems are well characterized. Numerous molecular dynamics and Monte Carlo simulations have been performed to determine their structure,[1–6] thermodynamic properties,[7–14] liquid-vapor phase behavior[15–22] and interfacial tension,[21,23–27] solid-liquid phase behavior,[28–31] solid-solid phase behavior,[32,33] and transport coefficients.[34–44]

The square-well model can also be extended to molecular systems by bonding atoms together via infinitely deep square-well potentials, as was first done by Rapaport.[45] These types of models have been used to investigate the properties of polymer systems,[46] including the freezing behavior of single square-well chains,[47,48] helix formation and aggregation,[49,50] coarse grained models for proteins,[51–53] and even for fibril formation by peptides.[54,55]

A slight generalization of the square-well potential is the discrete, or stepped, potential, which is composed of a sequence of square-wells/shoulders of various widths and depths. Stepped potentials can be used to approximate continuous potentials, such as the Lennard-Jones potential.[56,57] The number of steps can be adjusted to increase the accuracy or the computational speed of the representation. Force fields based on stepped potentials have been used to approximate the thermodynamics and phase behavior of "simple" molecules, such as step potentials for equilibria and discontinuous molecular dynamics (SPEADMD),[58,59] and even of peptide and protein solutions, such as PRIME.[54] In this article, we study square-well and square-shoulder systems (see Fig. 1) as they contain all the basic components of a stepped potential. The results obtained here are directly applicable to arbitrarily stepped potentials.

The dynamics of discrete potential systems is driven by events which occur when a pair of atoms are located at the edge of a "step" in the interaction potential (e.g., at $r=\sigma_{\alpha\alpha'}$ or $r=\lambda_{\alpha\alpha'}\sigma_{\alpha\alpha'}$ in Fig. 1). In the case of hard sphere systems, these events are just the collisions between the spheres. The static and dynamical properties of the system are completely specified by the rate of these events and their characteristics (e.g., the transfer of momentum, kinetic energy, etc.). For example, the pressure of a hard sphere system is directly related to the collision rate.[60] In this work, we examine the collision and velocity statistics of systems composed of stepped potential systems, which include the square-well and square-shoulder potentials. Specifically, we study the velocity distributions of atoms when they are undergoing an event,

a)Author to whom correspondence should be addressed. Electronic mail: marcus.bannerman@cbi.uni-erlangen.de.
b)Electronic mail: leo.lue@strath.ac.uk.

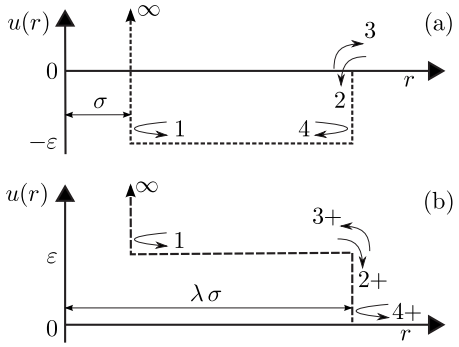

FIG. 1. Potential energy u as a function of atomic separation for a (a) square-well and (b) square-shoulder system. The arrows indicate the types of events occurring at the discontinuities in the potential (at $r=\sigma$ and $r=\lambda\sigma$) and are numbered as described in Sec. III.

which is different from the Maxwell–Boltzmann distribution. In addition, the rate of these events are explicitly related to thermodynamic properties of the system, such as the pressure and the temperature.

The remainder of this paper is organized as follows. The Maxwell–Boltzmann velocity distribution is quickly reviewed in Sec. II. Then in Sec. III, we review the different types of events that can occur between two square-well or square-shoulder atoms. Then the statistical properties of the atoms are examined while they undergo each of these types of events. In Sec. IV, these relative velocity distributions are then used to derive expressions for the kinetic energy of atoms immediately prior to each type of event. The rates of these events are related to the pair correlation function in Sec. V. This allow us to relate the temperature of the system to the event rates. In Sec. VI, the pressure is directly related to the event rates. Finally, in Sec. VII, the main results of the paper are summarized.

II. MAXWELL–BOLTZMANN VELOCITY STATISTICS

In a classical atomic system at equilibrium, the velocity $\mathbf{v}$ of each atom is distributed independently according to the Maxwell–Boltzmann distribution

$$f^{\mathrm{MB}}(\mathbf{v}) = \left(\frac{\beta m_\alpha}{2\pi}\right)^{3/2} e^{-\beta m_\alpha v^2/2}, \tag{2}$$

where m_α is the mass of the atom, $\beta=(k_B T)^{-1}$, k_B is the Boltzmann constant, and T is the absolute temperature. This is the probability density that a single atom has a particular velocity at any given moment.

Because the degrees of freedom corresponding to the momenta of the system are not coupled to the degrees of freedom corresponding to the positions, the velocity distribution of the atoms in the system are independent of each other. Consequently, the velocity distribution of a pair of atoms i (of type α) and j (of type α') is given by the product of the two single particle velocity distributions

$$f_{ij}(\mathbf{v}_i,\mathbf{v}_j) = f^{\mathrm{MB}}(\mathbf{v}_i) f^{\mathrm{MB}}(\mathbf{v}_j), \tag{3}$$

where $\mathbf{v}_i$ is the velocity of atom i and $\mathbf{v}_j$ is the velocity of atom j. The velocities of the pair of atoms can also be described in terms of the center of mass $\mathbf{V}_{ij}=(m_\alpha \mathbf{v}_i + m_{\alpha'}\mathbf{v}_j)/M_{\alpha\alpha'}$, where $M_{\alpha\alpha'}=m_\alpha+m_{\alpha'}$ is the total mass of the pair of atoms, and the relative velocity $\mathbf{v}_{ij}=\mathbf{v}_i-\mathbf{v}_j$ of the two atoms

$$f_{ij}^{\mathrm{MB}}(\mathbf{v}_i,\mathbf{v}_j) = f_{\mathrm{cm}}^{\mathrm{MB}}(\mathbf{V}_{ij}) f_{\mathrm{rel}}^{\mathrm{MB}}(\mathbf{v}_{ij}), \tag{4}$$

where

$$f_{\mathrm{cm}}^{\mathrm{MB}}(\mathbf{V}_{ij}) = \left(\frac{\beta M_{\alpha\alpha'}}{2\pi}\right)^{3/2} \exp\left(-\frac{\beta M_{\alpha\alpha'} V_{ij}^2}{2}\right), \tag{5}$$

and

$$f_{\mathrm{rel}}^{\mathrm{MB}}(\mathbf{v}_{ij}) = \left(\frac{\beta \mu_{\alpha\alpha'}}{2\pi}\right)^{3/2} \exp\left(-\frac{\beta \mu_{\alpha\alpha'} v_{ij}^2}{2}\right), \tag{6}$$

where $\mu_{\alpha\alpha'}=m_\alpha m_{\alpha'}/(m_\alpha+m_{\alpha'})$ is the reduced mass of the pair of atoms. Note that the relative and center-of-mass velocities are statistically independent of each other. Although these distributions are *on average* correct, the on-event distributions can differ significantly and are discussed in the following section.

III. ON-EVENT VELOCITY STATISTICS

The dynamics of discrete potential systems are driven by a series of events. In this section, we discuss the velocity distribution of a pair of atoms on an event. This distribution, in general, differs from the Maxwell–Boltzmann distribution, which was discussed in Sec. II. This is due to the fact that the rate at which an atom undergoes each type of event depends on its velocity and potential energy change.

Each event involves a pair of atoms i and j and occurs when they are separated by a distance corresponding to a discontinuity in the interaction potential. Between events, no forces act and these atoms have constant velocities $\mathbf{v}_i$ and $\mathbf{v}_j$. Upon execution of the event, the relative velocity of the atoms is instantaneously altered. The change in the relative velocity $\Delta\mathbf{v}_{ij}$ depends on the change in interaction energy $\Delta\varepsilon$ and the speed at which the atoms are moving toward each other. This speed is given by $b_{ij}=\hat{\mathbf{r}}_{ij}\cdot\mathbf{v}_{ij}$, where $\mathbf{r}_{ij}=\mathbf{r}_i-\mathbf{r}_j$ is a vector that points from the center of atom j to the center of atom i and $\hat{\mathbf{r}}_{ij}=\mathbf{r}_{ij}/|\mathbf{r}_{ij}|$ is the corresponding unit vector.

Before discussing the types of events in the square-well/shoulder system, we must first discuss the general collision rules. When two atoms encounter a discontinuity in the potential, they must have sufficient kinetic energy if they are to overcome the energy barrier $\Delta\varepsilon$. This condition can be expressed through

$$2\Delta\varepsilon/\mu_{\alpha\alpha'} \le b_{ij}^2. \tag{7}$$

If this expression holds true, the particles have sufficient energy to cross the discontinuity and their velocities are altered by

$$\begin{aligned} m_\alpha \Delta\mathbf{v}_i &= -m_{\alpha'}\Delta\mathbf{v}_j \\ &= -\mu_{\alpha\alpha'}\left[b_{ij} - \mathrm{sign}(b_{ij})\left(b_{ij}^2 - \frac{2\Delta\varepsilon}{\mu_{\alpha\alpha'}}\right)^{1/2}\right]\hat{\mathbf{r}}_{ij}. \end{aligned} \tag{8}$$

However, if the particles have insufficient energy to cross the discontinuity, then the particles undergo specular reflection

TABLE I. Parameters for the on-event distribution of the collision diameter.

k	Event type	$a^{(k)}_{\alpha\alpha'}$	$A^{(k)}_{\alpha\alpha'}$	$b^{(k)}_{ij,\min}$	$b^{(k)}_{ij,\max}$
1	Core	$\sigma^{+}_{\alpha\alpha'}$	-1	$-\infty$	0
2	Capture	$\lambda_{\alpha\alpha'}\sigma^{+}_{\alpha\alpha'}$	-1	$-\infty$	0
2+	Release	$\lambda_{\alpha\alpha'}\sigma^{-}_{\alpha\alpha'}$	1	0	∞
3	Disassociation	$\lambda_{\alpha\alpha'}\sigma^{-}_{\alpha\alpha'}$	$e^{\beta\varepsilon_{\alpha\alpha'}}$	$(2\varepsilon_{\alpha\alpha'}/\mu_{\alpha\alpha'})^{1/2}$	∞
3+	Association	$\lambda_{\alpha\alpha'}\sigma^{+}_{\alpha\alpha'}$	$-e^{\beta\varepsilon_{\alpha\alpha'}}$	$-\infty$	$-(2\varepsilon_{\alpha\alpha'}/\mu_{\alpha\alpha'})^{1/2}$
4	Bounce	$\lambda_{\alpha\alpha'}\sigma^{-}_{\alpha\alpha'}$	$(1-e^{-\beta\varepsilon_{\alpha\alpha'}})^{-1}$	0	$(2\varepsilon_{\alpha\alpha'}/\mu_{\alpha\alpha'})^{1/2}$
4+	Bounce	$\lambda_{\alpha\alpha'}\sigma^{+}_{\alpha\alpha'}$	$-(1-e^{-\beta\varepsilon_{\alpha\alpha'}})^{-1}$	$-(2\varepsilon_{\alpha\alpha'}/\mu_{\alpha\alpha'})^{1/2}$	0

$$m_\alpha \Delta \mathbf{v}_i = -m_{\alpha'}\Delta \mathbf{v}_j = -2\mu_{\alpha\alpha'} b_{ij}\hat{\mathbf{r}}_{ij}. \tag{9}$$

There are four different types of events that can occur between two square-well (square-shoulder) atoms: core, capture (association), disassociation (release), and bounce. These are well described in Ref. 61 and are also summarized below and in Fig. 1.

- **Type 1**, **Core:** A *core* event involves a collision between the hard cores of the two atoms. A core event occurs between two square-well/shoulder atoms when the distance between their centers becomes equal to their hard sphere event diameter $|\mathbf{r}_{ij}|=\sigma_{\alpha\alpha'}$. In addition, the spheres must be approaching each other, which implies that the event diameter must satisfy $b_{ij}<0$. These events are precisely the same as those that occur in the hard sphere system. As the potential energy change across the discontinuity is infinite ($\Delta\varepsilon\to\infty$), Eq. (7) is always false and the change of the velocities of the atoms after a core event is given by Eq. (9)
- **Type 2**, **Capture:** In a *capture* event, two square-well atoms become bound inside the attractive square-well. Immediately before a capture event, the centers of the square-well atoms initially lie outside the interaction well (i.e., $|\mathbf{r}_{ij}|=\lambda_{\alpha\alpha'}\sigma^{+}_{\alpha\alpha'}$). As the change in potential energy $\Delta\varepsilon=-\varepsilon_{\alpha\alpha'}$ is negative, Eq. (7) is always true and after the event, the atoms lie just inside the interaction well (i.e., $|\mathbf{r}_{ij}|=\lambda_{\alpha\alpha'}\sigma^{-}_{\alpha\alpha'}$). In addition, the spheres must be approaching each other (i.e., $b_{ij}<0$) for this event to occur.
- **Type** 2+, **Release:** A *release* event occurs for square-shoulder atoms when they exit each other's repulsive well ($|\mathbf{r}_{ij}|=\lambda_{\alpha\alpha'}\sigma^{-}_{\alpha\alpha'}\to\lambda_{\alpha\alpha'}\sigma^{+}_{\alpha\alpha'}$). The potential energy change $\Delta\varepsilon=-\varepsilon_{\alpha\alpha'}$ is again negative and Eq. (7) is always true; however, in this case, the collision diameter is restricted to receding atoms ($b_{ij}>0$).
- **Type 3**, **Disassociation:** In a *disassociation* event, two square-well atoms inside the attractive well are receding from each other with a relative velocity that is great enough to escape the attractive well ($|\mathbf{r}_{ij}|=\lambda_{\alpha\alpha'}\sigma^{-}_{\alpha\alpha'}\to\lambda_{\alpha\alpha'}\sigma^{+}_{\alpha\alpha'}$). The positive kinetic energy change ($\Delta\varepsilon=+\varepsilon_{\alpha\alpha'}$) and Eq. (7) restrict the event diameter to $(2\varepsilon_{\alpha\alpha'}/\mu_{\alpha\alpha'})^{1/2}\le b_{ij}\le\infty$ and if this is not satisfied, a type 4 bounce event occurs.
- **Type** 3+, **Association:** An *association* event occurs when two square-shoulder atoms approach each other with sufficient speed to enter the repulsive potential ($|\mathbf{r}_{ij}|=\lambda_{\alpha\alpha'}\sigma^{+}_{\alpha\alpha'}\to\lambda_{\alpha\alpha'}\sigma^{-}_{\alpha\alpha'}$). The collision diameter is then restricted to $-(2\varepsilon_{\alpha\alpha'}/\mu_{\alpha\alpha'})^{1/2}\ge b_{ij}\ge-\infty$ by Eq. (7) and $\Delta\varepsilon=+\varepsilon_{\alpha\alpha'}$; however, if this is not satisfied, a type 4+ bounce event occurs.
- **Type 4**, **Bounce:** In square-well systems, two particles undergo a *bounce* event when they are moving away from each other but their relative speed is too slow for them to escape the attractive well. Consequently, the event diameter is restricted to values in the range $0<b_{ij}<(2\varepsilon_{\alpha\alpha'}/\mu_{\alpha\alpha'})^{1/2}$.
- **Type** 4+, **Bounce:** For square-shoulder atoms, the bounce event occurs when the atoms approach each other but do not have a sufficient relative speed to overcome the repulsive interaction. This only occurs for collision diameters in the range $-(2\varepsilon_{\alpha\alpha'}/\mu_{\alpha\alpha'})^{1/2}<b_{ij}<0$.

In contrast to the velocities at a general time, the velocities of two atoms immediately prior to an event are not independent of each other, due to the constraints imposed by the impending event. In addition, they are also dependent on the relative separation and orientation (with respect to the relative velocity) of the atoms. However, the center-of-mass and relative velocities of the pair remain independent. Therefore, the distribution of the atom velocities $f^{(k)}_{ij}$ can be factored as

$$f^{(k)}_{ij}(\mathbf{v}_i,\mathbf{v}_j,\hat{\mathbf{r}}_{ij}) = f^{\mathrm{MB}}_{\mathrm{cm}}(\mathbf{V}_{ij}) p^{(k)}_{\mathrm{coll}}(\mathbf{v}_{ij},\hat{\mathbf{r}}_{ij}), \tag{10}$$

where $p^{(k)}_{\mathrm{coll}}$ is distribution of the relative velocity of two atoms on an event of type k.

The relative velocity is dependent on the relative orientation $\hat{\mathbf{r}}_{ij}$ of the atoms; however, the components of the relative velocity are independent of each other. It is convenient to consider the relative velocity in terms of the component parallel to $\hat{\mathbf{r}}_{ij}$ (i.e., b_{ij}) and the two components $v_{\perp,1}$ and $v_{\perp,2}$ perpendicular to $\hat{\mathbf{r}}_{ij}$. The perpendicular velocity components $v_{\perp,1}$ and $v_{\perp,2}$ are distributed according to the Maxwell–Boltzmann distribution [see Eq. (6)]. The collision diameter b_{ij} is also distributed according to the Maxwell–Boltzmann distribution; however, its values are restricted according to the type of event that the atoms undergo. Consequently, it is distributed according to

$$f^{(k)}(b_{ij}) = A^{(k)}\beta\mu_{\alpha\alpha'}b_{ij}e^{-\beta\mu_{\alpha\alpha'}b_{ij}^2/2}, \tag{11}$$

where $A^{(k)}$ is a normalization constant. A summary of the properties of each type of event is given in Table I. With this choice of variables, $p_{\text{coll}}^{(k)}$ can be written as

$$p_{\text{coll}}^{(k)}(\mathbf{v}_{ij},\hat{\mathbf{r}}_{ij})d\hat{\mathbf{r}}_{ij}d\mathbf{v}_{ij} = f^{(k)}(b_{ij})\frac{\beta\mu_{\alpha\alpha'}}{2\pi}e^{-\beta\mu_{\alpha\alpha'}(v_{\perp,1}^2+v_{\perp,2}^2)/2}d\hat{\mathbf{r}}_{ij}db_{ij}dv_{\perp,1}dv_{\perp,2}. \tag{12}$$

In Sec. IV, we will use this on-event velocity distribution to analyze the statistics of the kinetic energy of an atom on-event and then proceed to relate the event rates to the system pressure.

IV. ON-EVENT DISTRIBUTION OF THE KINETIC ENERGY

In this section, we determine the distribution $f_{\text{KE}}^{(k)}$ of the kinetic energy of an atom just prior to an event of type k. The atom is labeled i and its partner in the event is labeled j. The kinetic energy E_i of atom i can be determined from the velocity distribution of a pair of atoms on an event as

$$f_{\text{KE}}^{(k)}(\beta E_i) = \int d\hat{\mathbf{r}}_{ij}d\mathbf{v}_{ij}d\mathbf{V}_{ij}p_{\text{coll}}^{(k)}(\hat{\mathbf{r}}_{ij},\mathbf{v}_{ij})f_{\text{cm}}^{MB}(\mathbf{V}_{ij}) \times\delta\left(\beta E_i - \frac{\beta m_\alpha}{2}\left(V_{ij}^2 + 2\frac{\mu_{\alpha\alpha'}}{m_\alpha}\mathbf{V}_{ij}\cdot\mathbf{v}_{ij} + \left(\frac{\mu_{\alpha\alpha'}}{m_\alpha}\right)^2 v_{ij}^2\right)\right), \tag{13}$$

where E_i is the kinetic energy of atom i. Note that the speed distribution $f_{\text{coll}}^{(k)}$ of an atom just prior to an event of type k is directly related to $f_{\text{KE}}^{(k)}$ as

$$f_{\text{coll}}^{(k)}(v_i) = \beta m_\alpha v_i f_{\text{KE}}^{(k)}\left(\frac{\beta m_\alpha v_i^2}{2}\right).$$

The integral in Eq. (13) is difficult to evaluate directly; however, progress can be made if we work with the Laplace transform of the kinetic energy distribution $\tilde{f}_{\text{KE}}^{(k)}$, which is defined as

$$\tilde{f}_{\text{KE}}^{(k)}(s) = \int_0^\infty d\beta E e^{-s\beta E}f_{\text{KE}}^{(k)}(\beta E).$$

This can be determined as

$$\begin{aligned}
\tilde{f}_{\text{KE}}^{(k)}(s) &= \int d\hat{\mathbf{r}}_{ij}d\mathbf{v}_{ij}d\mathbf{V}_{ij}p_{\text{coll}}^{(k)}(\hat{\mathbf{r}}_{ij},\mathbf{v}_{ij})f_{\text{cm}}^{MB}(\mathbf{V}_{ij})\exp\left[-s\frac{\beta m_\alpha}{2}\left(V_{ij}^2 + 2\frac{\mu_{\alpha\alpha'}}{m_\alpha}\mathbf{V}_{ij}\cdot\mathbf{v}_{ij} + \left(\frac{\mu_{\alpha\alpha'}}{m_\alpha}\right)^2 v_{ij}^2\right)\right] \\
&= \left(\frac{M_{\alpha\alpha'}/m_\alpha}{s+M_{\alpha\alpha'}/m_\alpha}\right)^{3/2}\int d\hat{\mathbf{r}}_{ij}d\mathbf{v}_{ij}p_{\text{coll}}^{(k)}(\hat{\mathbf{r}}_{ij},\mathbf{v}_{ij})\exp\left[-\frac{sM_{\alpha\alpha'}/m_\alpha}{s+M_{\alpha\alpha'}/m_\alpha}\frac{\beta\mu_{\alpha\alpha'}^2 v_{ij}^2}{2m_\alpha}\right] \\
&= \left(\frac{M_{\alpha\alpha'}/m_\alpha}{s+M_{\alpha\alpha'}/m_\alpha}\right)^{3/2}\int_0^\infty dv_\perp v_\perp\int_{b_{ij,\min}^{(k)}}^{b_{ij,\max}^{(k)}} db_{ij}A^{(k)}(\beta\mu_{\alpha\alpha'})^2 b_{ij}\exp\left[-\frac{\beta\mu_{\alpha\alpha'}}{2}(b_{ij}^2+v_\perp^2) - \frac{sM_{\alpha\alpha'}/m_\alpha}{s+M_{\alpha\alpha'}/m_\alpha}(b_{ij}^2+v_\perp^2)\frac{\beta\mu_{\alpha\alpha'}^2}{2m_\alpha}\right] \\
&= A^{(k)}\left(\frac{m_\alpha}{M_{\alpha\alpha'}}\right)^{1/2}\frac{(s+M_{\alpha\alpha'}/m_\alpha)^{1/2}}{(s+1)^2}\left\{\exp\left[-\frac{\beta m_{\alpha'}}{2}\left(\frac{s+1}{s+M_{\alpha\alpha'}/m_\alpha}\right)(b_{ij,\min}^{(k)})^2\right] - \exp\left[-\frac{\beta m_{\alpha'}}{2}\left(\frac{s+1}{s+M_{\alpha\alpha'}/m_\alpha}\right)(b_{ij,\max}^{(k)})^2\right]\right\}.
\end{aligned} \tag{14}$$

The general form of the Laplace transform of the kinetic energy distribution of an atom immediately prior to an event is the same for each type of event; only the values of the parameters $A^{(k)}$, $b_{ij,\min}^{(k)}$, and $b_{ij,\max}^{(k)}$, which can be found in Table I, differ. This expression is independent of the size of the colliding atoms or the density of the system. However, the kinetic energy distribution of atom i does depend on the mass $m_{\alpha'}$ of its collision partner. As a comparison, the corresponding expression for the Laplace transform of the Maxwell–Boltzmann distribution is

$$\tilde{f}_{\text{KE}}^{\text{MB}}(s) = (s+1)^{-3/2}. \tag{15}$$

The Laplace transform of the kinetic energy distribution also allows for the convenient calculations of the moments of the distribution

$$\langle(\beta E_i)^n\rangle^{(k)} = (-1)^n\frac{\partial^n\tilde{f}_{\text{MB}}^{(k)}(0)}{\partial s^n},$$

where $\langle\cdots\rangle^{(k)}$ is an average over events of type k.

In the remainder of this section, we will examine in more detail the behavior of the kinetic energy distribution for atoms on each type of event. All results are validated against results obtained from event-driven simulations in the canonical (NVT) and microcanonical (NVE) ensemble. All systems, if not otherwise specified, consisted of 32 000 atoms at a temperature/well energy of $\beta\varepsilon=1$, a well width of $\lambda=1.5$, and a number density of $N/V=1.1$. Multicomponent systems consisted of equal numbers of the two atom species, simulated over a range of mass ratios. The NVT simulations utilized an Andersen thermostat which accounted for around

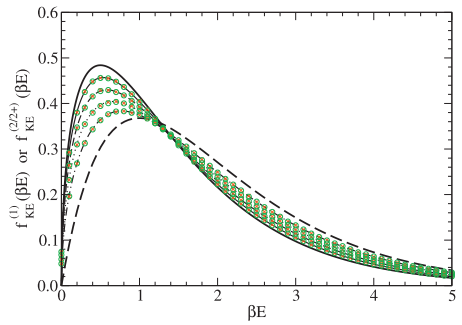

FIG. 2. Kinetic energy distribution for an atom of mass m_α on a core, a capture, or a release event with an atom of mass $m_{\alpha'}$ in a multicomponent square-well/shoulder system, where (i) $m_{\alpha'}/m_\alpha=0.2$ (solid line), (ii) $m_{\alpha'}/m_\alpha=0.5$ (long dashed line), (iii) $m_{\alpha'}/m_\alpha=1$ (dotted line), (iv) $m_{\alpha'}/m_\alpha=2$ (dashed-dotted line), and (v) $m_{\alpha'}/m_\alpha\to\infty$ (thick dashed line). The thick solid line is the result of the Maxwell–Boltzmann distribution, which also corresponds to the case $m_{\alpha'}/m_\alpha=0$. The circles are from NVE MD simulations and the crosses are from NVT MD simulations for core events.

5% of the total number of events. NVT simulations were run for an equilibration period of 2×10^7 events before data were collected over 2×10^7 events. NVE simulations used the output of the NVT simulations with the thermostat disabled and exhibited a temperature within 0.5% of the NVT temperature. These were then run for 2×10^7 events to collect statistical data. The energy histograms were collected using a bin width of $\beta\varepsilon=0.1$.

A. Core event

For an atom on a core event, the Laplace transform of the kinetic energy distribution is

$$\tilde{f}_{\mathrm{KE}}^{(1)}(s)=\left(\frac{m_\alpha}{M_{\alpha\alpha'}}\right)^{1/2}\frac{(s+M_{\alpha\alpha'}/m_\alpha)^{1/2}}{(s+1)^2}. \tag{16}$$

This is precisely the same form as found for hard spheres on a collision in three dimensions.[60] The inverse Laplace transform can be performed analytically (see Appendix) to give

$$\begin{aligned}f_{\mathrm{KE}}^{(1)}(\beta E)&=\left(\frac{m_\alpha}{M_{\alpha\alpha'}}\right)^{1/2}h_0(\beta E,M_{\alpha\alpha'}/m_\alpha)\\&=\left(\frac{m_\alpha}{M_{\alpha\alpha'}}\right)^{1/2}(\beta E)^{1/2}\left[\frac{e^{-(m_{\alpha'}/m_\alpha)\beta E}}{\pi^{1/2}}\right.\\&\left.+\frac{1+2(m_{\alpha'}/m_\alpha)\beta E}{2[(m_{\alpha'}/m_\alpha)\beta E]^{1/2}}\mathrm{erf}\left(\left(\frac{m_{\alpha'}}{m_\alpha}\beta E\right)^{1/2}\right)\right]e^{-\beta E}.\end{aligned} \tag{17}$$

The shape of the distribution of βE is independent of the temperature, density, and composition of the system. It does, however, depend on the relative masses of the colliding pair of atoms. The kinetic energy distribution of an atom on a core event is plotted in Fig. 2 for collision partners of different masses. The lines are the predictions of Eq. (17) and the symbols are from event-driven molecular dynamics simulations. As the mass of the collision partner increases, the on-collision kinetic energy of the atom shifts to higher values. The kinetic energy of an atom on a core event is generally higher than that of the Maxwell–Boltzmann distribution. The thick solid line is the Maxwell–Boltzmann distribution, which is the inverse Laplace transform of Eq. (15)

$$f_{\mathrm{KE}}^{\mathrm{MB}}(\beta E)=\frac{2}{\pi^{1/2}}(\beta E)^{1/2}e^{-\beta E}. \tag{18}$$

The thick dashed line is the on-collision kinetic energy distribution for an atom in the limit that the collision partner has an infinite mass.

The on-collision distribution differs from the Maxwell–Boltzmann distribution because atoms that move faster collide more frequently. Consequently, these atoms are "sampled" more often than the slower moving atoms, and, therefore, the on-collision distribution is shifted to higher values of the kinetic energy.

As the relative mass of the partner atom j increases, the kinetic energy of the atom i increases. The mean kinetic energy of an atom on a core event is

$$\langle\beta E\rangle^{(1)}=2-\frac{1}{2}\left(\frac{m_\alpha}{M_{\alpha\alpha'}}\right),$$

which is greater the Maxwell–Boltzmann value $\langle\beta E\rangle^{\mathrm{MB}}=3/2$.

In the limit that the mass of the collision partner is much smaller than the mass of the atom (i.e., $m_{\alpha'}/m_\alpha\to0$), the on-event kinetic energy distribution approaches the Maxwell–Boltzmann distribution. This can be understood by the fact that a collision with a massless particle will not affect the trajectory of an atom.

Pairs of atoms with a higher relative speed will collide more often. The mean speed of an atom will decrease as its mass increases. Therefore, as the mass of the collision partner j of an atom i increases, thereby "slowing" down, atom i must itself be faster to provide the same relative speed. This explains the shift of the distribution to higher kinetic energies with increasing mass of the collision partner. As the mass of the collision partner becomes much greater than the mass of the atom (i.e., $m_{\alpha'}/m_\alpha\gg1$), the distribution shifts to lower values of the kinetic energy and eventually approaches

$$f_{\mathrm{KE}}^{(1)}(\beta E)\to\beta E e^{-\beta E}.$$

This corresponds to the collision of a particle with an infinitely massive particle or with an immovable surface.

B. Capture and release events

The kinetic energy distribution of a particle on a capture event is identical to that for an atom on a core event [see Eq. (17)]. This is also the case for atoms prior to a release event in the case of square-shoulder atoms. Both these distributions are plotted in Fig. 2 for an atom with collision partners of differing masses.

C. Disassociation and association events

For an association event for square-shoulder systems, the kinetic energy distribution is identical to that for atoms on a disassociation event. For an atom immediately prior to a disassociation or association event, Eq. (14) becomes

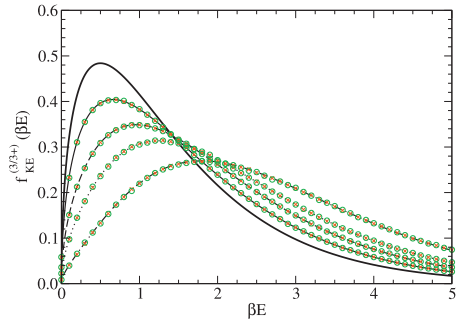

FIG. 3. Kinetic energy distribution for atoms on a disassociation or association event in a single component square-well/shoulder system with (i) $\beta\varepsilon_{\alpha\alpha'}=0$ (solid line), (ii) $\beta\varepsilon_{\alpha\alpha'}=0.5$ (dashed line), (iii) $\beta\varepsilon_{\alpha\alpha'}=1.0$ (dotted line), and (iv) $\beta\varepsilon_{\alpha\alpha'}=2.0$ (dashed-dotted line). The thick solid line is the result of the Maxwell–Boltzmann distribution. The circles are from NVE MD simulations and the crosses are from NVT MD simulations for disassociation events.

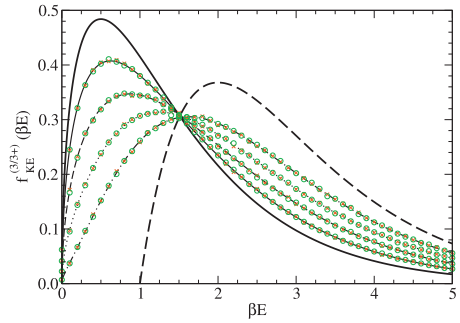

FIG. 4. Kinetic energy distribution for an atom of mass m_α on a disassociation or association event with an atom of mass $m_{\alpha'}$ in a multicomponent square-well/shoulder system with $\beta\varepsilon_{\alpha\alpha'}=1$, where (i) $m_{\alpha'}/m_\alpha=0.2$ (solid line), (ii) $m_{\alpha'}/m_\alpha=0.5$ (long dashed line), (iii) $m_{\alpha'}/m_\alpha=1$ (dotted line), (iv) $m_{\alpha'}/m_\alpha=2$ (dashed-dotted line), and (v) $m_{\alpha'}/m_\alpha\to\infty$ (thick dashed line). The thick solid line is the result of the Maxwell–Boltzmann distribution, which also corresponds to the case $m_{\alpha'}/m_\alpha=0$. The circles are from NVE MD simulations and the crosses are from NVT MD simulations for disassociation events.

$$\tilde{f}_{\mathrm{KE}}^{(3)}(s)=e^{\beta\varepsilon_{\alpha\alpha'}}\left(\frac{m_\alpha}{M_{\alpha\alpha'}}\right)^{1/2}\frac{(s+M_{\alpha\alpha'}/m_\alpha)^{1/2}}{(s+1)^2}\times\exp\left[-\beta\varepsilon_{\alpha\alpha'}\left(\frac{M_{\alpha\alpha'}}{m_\alpha}\right)\left(\frac{s+1}{s+M_{\alpha\alpha'}/m_\alpha}\right)\right]. \quad (19)$$

This expression can be inverted analytically to yield

$$f_{\mathrm{KE}}^{(3)}(\beta E)=\left(\frac{m_\alpha}{M_{\alpha\alpha'}}\right)^{1/2}e^{\beta\varepsilon_{\alpha\alpha'}}h_0(\beta E;M_{\alpha\alpha'}/m_\alpha)-\beta\varepsilon_{\alpha\alpha'}\left(\frac{M_{\alpha\alpha'}}{m_\alpha}\right)^{1/2}e^{\beta\varepsilon_{\alpha\alpha'}}h_1(\beta E;M_{\alpha\alpha'}/m_\alpha)+\left(\frac{m_\alpha}{M_{\alpha\alpha'}}\right)^{1/2}e^{\beta\varepsilon_{\alpha\alpha'}}h_2(\beta E;M_{\alpha\alpha'}/m_\alpha,\beta\varepsilon_{\alpha\alpha'},M_{\alpha\alpha'}/m_\alpha), \quad (20)$$

where the function h_1 is defined in Eq. (A4) and the function h_2 is defined in Eq. (A6).

The distribution of the kinetic energy of a square-well atom prior to a disassociation or association event is shown in Fig. 3 for a single component square-well/shoulder system at various temperatures. The lines are from Eq. (20) and the symbols are from constant energy and constant temperature molecular dynamics simulations at various densities. As expected, the analytical formula agrees with the simulation results to within the statistical uncertainty of the data.

The kinetic energy of an atom on a core event is generally higher than that of the Maxwell–Boltzmann distribution. The mean kinetic energy of an atom on a disassociation event is

$$\langle\beta E\rangle^{(3)}=2-\frac{1}{2}\left(\frac{m_\alpha}{M_{\alpha\alpha'}}\right)+\beta\varepsilon_{\alpha\alpha'}\left[1-\left(\frac{m_\alpha}{M_{\alpha\alpha'}}\right)\right],$$

which is higher than on either a core or capture event. This is because the atom must be moving away from its event partner at a sufficiently high speed to escape the attractive well.

In the limit when $\beta\varepsilon_{\alpha\alpha'}\to 0$ (i.e., the high temperature limit), the kinetic energy distribution approaches that of a core or capture event. This is expected, as in this situation the atom will, in general, have a large kinetic energy, and the attractive well becomes irrelevant.

In Fig. 4, the kinetic energy distribution of an atom on a disassociation event in a multicomponent square-well system at $\beta\varepsilon_{\alpha\alpha'}=1$ is plotted for collision partners of differing masses. The lines are the predictions of Eq. (20) and the symbols are from molecular dynamics simulations. When the mass of the atom i is much larger than its collision partner j (i.e., $m_{\alpha'}/m_\alpha\to 0$), the distribution approaches the Maxwell–Boltzmann distribution, which is the same as in the case of the core and capture events. When the mass of the atom i is much smaller than its collision partner, the kinetic energy distribution approaches

$$f^{(3)}(\beta E)\to\Theta(E-\varepsilon_{\alpha\alpha'})(\beta E-\beta\varepsilon_{\alpha\alpha'})e^{\beta E-\beta\varepsilon_{\alpha\alpha'}},$$

where Θ is the Heaviside step function. This limit corresponds to the escape of an atom from the attractive well of a stationary object, such as a wall. Unless the atom has a kinetic energy greater than the depth of the attractive well, it cannot disassociate.

D. Bounce events

The statistics of the kinetic energy for square-shoulder atoms on a bounce event are the same as that for square-well atoms on a bounce event. The Laplace transform of the kinetic energy distribution of an atom on a bounce event is given by

$$\tilde{f}_{\mathrm{KE}}^{(4)}(s)=\frac{(m_\alpha/M_{\alpha\alpha'})^{1/2}}{1-e^{-\beta\varepsilon_{\alpha\alpha'}}}\frac{(s+M_{\alpha\alpha'}/m_\alpha)^{1/2}}{(s+1)^2}\times\left\{1-\exp\left[-\beta\varepsilon_{\alpha\alpha'}\left(\frac{M_{\alpha\alpha'}}{m_\alpha}\right)\left(\frac{s+1}{s+M_{\alpha\alpha'}/m_\alpha}\right)\right]\right\}. \quad (21)$$

The corresponding expression for the kinetic energy distribution is

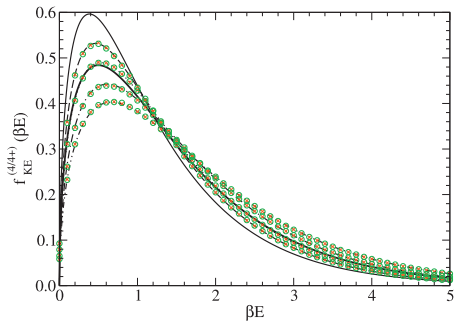

FIG. 5. Kinetic energy distribution for atoms on a bounce event in a single component square-well/shoulder system with (i) $\beta\varepsilon_{\alpha\alpha'}=0$ (solid line), (ii) $\beta\varepsilon_{\alpha\alpha'}=0.5$ (long dashed line), (iii) $\beta\varepsilon_{\alpha\alpha'}=1.0$ (dotted line), (iv) $\beta\varepsilon_{\alpha\alpha'}=2.0$ (dashed-dotted line), and (v) $\beta\varepsilon_{\alpha\alpha'}\to\infty$ (dashed-dotted-dotted line). The thick solid line is the result of the Maxwell–Boltzmann distribution. The circles are from NVE MD simulations and the crosses are from NVT MD simulations.

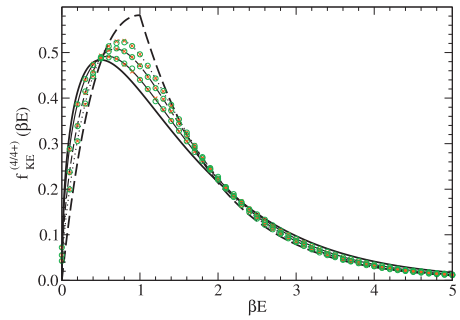

FIG. 6. Kinetic energy distribution for an atom of mass m_α on a bounce event with an atom of mass $m_{\alpha'}$ in a multicomponent square-well system with $\beta\varepsilon_{\alpha\alpha'}=1$, where (i) $m_{\alpha'}/m_\alpha=2$ (solid line), (ii) $m_{\alpha'}/m_\alpha=5$ (long dashed line), (iii) $m_{\alpha'}/m_\alpha=10$ (dotted line), and (iv) $m_{\alpha'}/m_\alpha\to\infty$ (thick dashed line). The thick solid line is the result of the Maxwell–Boltzmann distribution, which also corresponds to the case $m_{\alpha'}/m_\alpha=0$.

$$f_{\mathrm{KE}}^{(4)}(\beta E)=\frac{(M_{\alpha\alpha'}/m_\alpha)^{1/2}}{1-e^{-\beta\varepsilon_{\alpha\alpha'}}}\beta\varepsilon_{\alpha\alpha'}h_1(\beta E;M_{\alpha\alpha'}/m_\alpha)-\frac{(m_\alpha/M_{\alpha\alpha'})^{1/2}}{1-e^{-\beta\varepsilon_{\alpha\alpha'}}}h_2(\beta E;M_{\alpha\alpha'}/m_\alpha,\beta\varepsilon_{\alpha\alpha'}M_{\alpha\alpha'}/m_\alpha).$$

The distribution of the kinetic energy of an atom prior to a bounce event is given in Fig. 5 for a single component square-well/shoulder system at various temperatures. The lines are the predictions of Eq. (22) and the symbols are from molecular dynamics simulations. The two agree within the statistical uncertainty of the simulation data.

At high temperatures (i.e., $\beta\varepsilon_{\alpha\alpha'}<1$), the kinetic energy distribution of an atom on a bounce event is shifted to lower values than the Maxwell–Boltzmann distribution. In this situation, the atom typically has sufficient kinetic energy to escape the attractive well; therefore, atoms on a bounce event will have a lower than average kinetic energy. At low temperatures (i.e., $\beta\varepsilon_{\alpha\alpha'}>1$), the kinetic energy distribution is shifted to higher values than that of the Maxwell–Boltzmann distribution.

The mean kinetic energy of an atom on a bounce event is

$$\langle\beta E\rangle^{(4)}=2-\frac{1}{2}\left(\frac{m_\alpha}{M_{\alpha\alpha'}}\right)-\frac{\beta\varepsilon_{\alpha\alpha'}}{e^{\beta\varepsilon_{\alpha\alpha'}}-1}\left[1-\left(\frac{m_\alpha}{M_{\alpha\alpha'}}\right)\right].$$

In the high temperature limit, this becomes

$$f_{\mathrm{KE}}^{(4)}(\beta E)\approx\left(\frac{M_{\alpha\alpha'}}{m_\alpha}\right)^{1/2}e^{-\beta E}\,\mathrm{erf}\left(\left(\frac{m_{\alpha'}}{m_\alpha}\beta E\right)^{1/2}\right)+\cdots.$$

In the low temperature limit (i.e., $\beta\varepsilon_{\alpha\alpha'}\to\infty$), the kinetic energy distribution approaches that of the core or capture events [see Eq. (17)]. In this limit, the atom will never have sufficient kinetic energy to escape the attractive well and the captured atoms become bonded as in Rapaport's[45] model for polymers.

The kinetic energy distribution for an atom on a bounce event with partners of various masses in a multicomponent square-well system at $\beta\varepsilon_{\alpha\alpha'}=1$ is shown in Fig. 6. In the limit that the mass of atom i is much larger than the mass of its partner on a bounce event, the kinetic distribution approaches that of the Maxwell–Boltzmann distribution. In the limit that the mass of atom i is much smaller than its event partner, the distribution approaches

$$f_{\mathrm{KE}}^{(4)}(\beta E)\approx\beta[E+(\varepsilon_{\alpha\alpha'}-E)\Theta(E-\varepsilon_{\alpha\alpha'})]\frac{e^{-\beta E}}{1-e^{-\beta\varepsilon_{\alpha\alpha'}}}.$$

E. Summary

Exact analytic expressions have been developed for the distribution of the kinetic energy of an atom immediately prior to undergoing an event with another partner atom; these have been validated with molecular dynamics (MD) simulation data. The on-event kinetic energy distributions are easily collected in an event-driven MD simulation and, combined with the above analytical expressions, they offer a sensitive method for checking if a system has been equilibrated.

V. THE PAIR CORRELATION FUNCTION

In this section, we relate the event rates to the pair correlation functions between atoms. This will provide an expression for the discontinuity in the pair correlation function for square-well and square-shoulder systems. It will also lead to a relationship between the temperature of a system and the event rates.

Let us determine the average number of events that a particular atom i of type α experiences in a small interval of time Δt with atoms of type α'. Consider an atom j of type α' which is moving from atom i with a speed $b_{ij}=\hat{\mathbf{r}}_{ij}\cdot\mathbf{v}_{ij}$. This atom must be within a distance $|b_{ij}|\Delta t+a_{\alpha\alpha'}^{(k)}$ from the center of atom i if it is to participate in an event of type k with it within a time Δt. The number of these atoms which will collide with atom i is then

$$\Delta\mathcal{N}_{\alpha\alpha'}^{(k)}(b_{ij})=\rho_{\alpha'}g_{\alpha\alpha'}(a_{\alpha\alpha'}^{(k)})f_{\mathrm{rel}}^{\mathrm{MB}}(b_{ij})4\pi[a_{\alpha\alpha'}^{(k)}]^2|b_{ij}|\Delta t, \tag{22}$$

where $g_{\alpha\alpha'}$ is the pair correlation function.

To get the total number of atoms of type α' which will collide with a particular atom of type α, we just need to integrate this expression over all allowable values of the collision diameter b_{ij}. Thus, the mean number $\Delta\mathcal{N}_{\alpha\alpha'}^{(k)}$ of type k

events experienced by a single atom of type α with atoms of type α' in a small interval of time Δt is given by

$$\Delta\mathcal{N}_{\alpha\alpha'}^{(k)} = \rho_{\alpha'} g_{\alpha\alpha'}(a_{\alpha\alpha'}^{(k)}) 4\pi [a_{\alpha\alpha'}^{(k)}]^2 \int_{b_{ij,\min}^{(k)}}^{b_{ij,\max}^{(k)}} \mathrm{d}b_{ij} |b_{ij}| \times \left(\frac{\beta\mu_{\alpha\alpha'}}{2\pi}\right)^{1/2} e^{-\beta\mu_{\alpha\alpha'} b_{ij}^2/2} \Delta t. \quad (23)$$

The total number $\mathcal{N}_{\alpha\alpha'}^{(k)}$ of events of type k in the system between atoms of type α and type α' in an interval of time τ is then

$$\mathcal{N}_{\alpha\alpha'}^{(k)} = \frac{N_\alpha \tau}{1+\delta_{\alpha\alpha'}} \frac{\Delta\mathcal{N}_{\alpha\alpha'}}{\Delta t},$$

where N_α is the number of atoms of type α in the system and $\delta_{\alpha\alpha'}$ is the Kronecker delta function. The factor $1+\delta_{\alpha\alpha'}$ prevents the double counting of events between atoms of the same type.

Therefore, the rate of core, capture, disassociation, and bounce events are

$$\frac{\mathcal{N}_{\alpha\alpha'}^{(1)}}{N\tau} = \frac{4\pi\rho x_\alpha x_{\alpha'}}{(1+\delta_{\alpha\alpha'})} \sigma_{\alpha\alpha'}^3 g_{\alpha\alpha'}(\sigma_{\alpha\alpha'}^+) (2\pi\beta\mu_{\alpha\alpha'}\sigma_{\alpha\alpha'}^2)^{-1/2}, \quad (24)$$

$$\frac{\mathcal{N}_{\alpha\alpha'}^{(2)}}{N\tau} = \frac{4\pi\rho x_\alpha x_{\alpha'}}{(1+\delta_{\alpha\alpha'})} (\lambda_{\alpha\alpha'}\sigma_{\alpha\alpha'})^3 g_{\alpha\alpha'}(\lambda_{\alpha\alpha'}\sigma_{\alpha\alpha'}^+) \times (2\pi\beta\mu_{\alpha\alpha'}\lambda_{\alpha\alpha'}^2\sigma_{\alpha\alpha'}^2)^{-1/2}, \quad (25)$$

$$\frac{\mathcal{N}_{\alpha\alpha'}^{(3)}}{N\tau} = \frac{4\pi\rho x_\alpha x_{\alpha'}}{(1+\delta_{\alpha\alpha'})} (\lambda_{\alpha\alpha'}\sigma_{\alpha\alpha'})^3 g_{\alpha\alpha'}(\lambda_{\alpha\alpha'}\sigma_{\alpha\alpha'}^-) \times \frac{e^{-\beta\varepsilon_{\alpha\alpha'}}}{(2\pi\beta\mu_{\alpha\alpha'}\lambda_{\alpha\alpha'}^2\sigma_{\alpha\alpha'}^2)^{1/2}}, \quad (26)$$

$$\frac{\mathcal{N}_{\alpha\alpha'}^{(4)}}{N\tau} = \frac{4\pi\rho x_\alpha x_{\alpha'}}{(1+\delta_{\alpha\alpha'})} (\lambda_{\alpha\alpha'}\sigma_{\alpha\alpha'})^3 g_{\alpha\alpha'}(\lambda_{\alpha\alpha'}\sigma_{\alpha\alpha'}^-) \times \frac{1-e^{-\beta\varepsilon_{\alpha\alpha'}}}{(2\pi\beta\mu_{\alpha\alpha'}\lambda_{\alpha\alpha'}^2\sigma_{\alpha\alpha'}^2)^{1/2}}, \quad (27)$$

where N is the total number of atoms in the system and $x_\alpha = N_\alpha/N$ is the mole fraction of atoms of type α in the system. These equations can be used to determine the value of the pair correlation functions in terms of the event rates

$$g_{\alpha\alpha'}(\sigma_{\alpha\alpha'}^+) = (1+\delta_{\alpha\alpha'}) \frac{(2\pi\beta\mu_{\alpha\alpha'}\sigma_{\alpha\alpha'}^2)^{1/2}}{4\pi\rho x_\alpha x_{\alpha'}\sigma_{\alpha\alpha'}^3} \frac{\mathcal{N}_{\alpha\alpha'}^{(1)}}{N\tau}, \quad (28)$$

$$g_{\alpha\alpha'}(\lambda_{\alpha\alpha'}\sigma_{\alpha\alpha'}^+) = (1+\delta_{\alpha\alpha'}) \frac{(2\pi\beta\mu_{\alpha\alpha'}\lambda_{\alpha\alpha'}^2\sigma_{\alpha\alpha'}^2)^{1/2}}{4\pi\rho x_\alpha x_{\alpha'}\lambda_{\alpha\alpha'}^3\sigma_{\alpha\alpha'}^3} \frac{\mathcal{N}_{\alpha\alpha'}^{(2)}}{N\tau}, \quad (29)$$

$$g_{\alpha\alpha'}(\lambda_{\alpha\alpha'}\sigma_{\alpha\alpha'}^-) = (1+\delta_{\alpha\alpha'}) \frac{(2\pi\beta\mu_{\alpha\alpha'}\lambda_{\alpha\alpha'}^2\sigma_{\alpha\alpha'}^2)^{1/2}}{4\pi\rho x_\alpha x_{\alpha'}\lambda_{\alpha\alpha'}^3\sigma_{\alpha\alpha'}^3} \times e^{\beta\varepsilon_{\alpha\alpha'}} \frac{\mathcal{N}_{\alpha\alpha'}^{(3)}}{N\tau}, \quad (30)$$

$$g_{\alpha\alpha'}(\lambda_{\alpha\alpha'}\sigma_{\alpha\alpha'}^-) = (1+\delta_{\alpha\alpha'}) \frac{(2\pi\beta\mu_{\alpha\alpha'}\lambda_{\alpha\alpha'}^2\sigma_{\alpha\alpha'}^2)^{1/2}}{4\pi\rho x_\alpha x_{\alpha'}\lambda_{\alpha\alpha'}^3\sigma_{\alpha\alpha'}^3} \times \frac{e^{\beta\varepsilon_{\alpha\alpha'}}}{(e^{\beta\varepsilon_{\alpha'}}-1)} \frac{\mathcal{N}_{\alpha\alpha'}^{(4)}}{N\tau}. \quad (31)$$

These expressions have been previously developed by Einwohner and Alder[62] for single component systems. Identical expressions exist for square-shoulder systems.

$$g_{\alpha\alpha'}(\lambda_{\alpha\alpha'}\sigma_{\alpha\alpha'}^-) = (1+\delta_{\alpha\alpha'}) \frac{(2\pi\beta\mu_{\alpha\alpha'}\lambda_{\alpha\alpha'}^2\sigma_{\alpha\alpha'}^2)^{1/2}}{4\pi\rho x_\alpha x_{\alpha'}\lambda_{\alpha\alpha'}^3\sigma_{\alpha\alpha'}^3} \frac{\mathcal{N}_{\alpha\alpha'}^{(2+)}}{N\tau}, \quad (32)$$

$$g_{\alpha\alpha'}(\lambda_{\alpha\alpha'}\sigma_{\alpha\alpha'}^+) = (1+\delta_{\alpha\alpha'}) \frac{(2\pi\beta\mu_{\alpha\alpha'}\lambda_{\alpha\alpha'}^2\sigma_{\alpha\alpha'}^2)^{1/2}}{4\pi\rho x_\alpha x_{\alpha'}\lambda_{\alpha\alpha'}^3\sigma_{\alpha\alpha'}^3} \times e^{\beta\varepsilon_{\alpha\alpha'}} \frac{\mathcal{N}_{\alpha\alpha'}^{(3+)}}{N\tau}, \quad (33)$$

$$g_{\alpha\alpha'}(\lambda_{\alpha\alpha'}\sigma_{\alpha\alpha'}^+) = (1+\delta_{\alpha\alpha'}) \frac{(2\pi\beta\mu_{\alpha\alpha'}\lambda_{\alpha\alpha'}^2\sigma_{\alpha\alpha'}^2)^{1/2}}{4\pi\rho x_\alpha x_{\alpha'}\lambda_{\alpha\alpha'}^3\sigma_{\alpha\alpha'}^3} \times \frac{e^{\beta\varepsilon_{\alpha\alpha'}}}{(e^{\beta\varepsilon_{\alpha'}}-1)} \frac{\mathcal{N}_{\alpha\alpha'}^{(4+)}}{N\tau}. \quad (34)$$

In the more general case of systems where the atoms interact through a stepped potential, these expressions relate the value of the pair correlation function directly before or after the various steps of the potential to the rate of capture, disassociation, and bounce (or release, association, and bounce) events across the steps.

At equilibrium, the interaction energy of the system must remain constant on average. As a consequence, the number of capture events must equal the number of disassociation events (i.e., $\mathcal{N}_{\alpha\alpha'}^{(2)} = \mathcal{N}_{\alpha\alpha'}^{(3)}$) at long times. By comparing Eqs. (29) and (30) [or Eqs. (32) and (33) in the case of square-shoulder systems], the values of the pair correlation function just inside and outside the interaction well are related by

$$g_{\alpha\alpha'}(\lambda_{\alpha\alpha'}\sigma_{\alpha\alpha'}^-) = e^{\beta\varepsilon_{\alpha\alpha'}} g_{\alpha\alpha'}(\lambda_{\alpha\alpha'}\sigma_{\alpha\alpha'}^+). \quad (35)$$

This relationship can also be derived from the requirement of the continuity of the indirect correlation function.[63]

Equations (30) and (31) impose a relationship between the disassociation and bounce event rates in the system

$$\mathcal{N}_{\alpha\alpha'}^{(4)} = (e^{\beta\varepsilon_{\alpha\alpha'}} - 1)\mathcal{N}_{\alpha\alpha'}^{(3)}. \quad (36)$$

In the case of square-shoulder systems, an identical relationship holds between the number of association and the bounce

events. If the temperature of the system, or equivalently β, were known, then the dissociation and bounce event rates are not independent. Therefore, we conclude there are only two independent event rates in single component square-well or square-shoulder systems: the core and the bounce event rates.

In addition, this allows the calculation of the temperature of the system directly from knowledge of only the event rates

$$\beta\varepsilon_{\alpha\alpha'} = \ln\left(1 + \frac{\mathcal{N}^{(4)}_{\alpha\alpha'}}{\mathcal{N}^{(3)}_{\alpha\alpha'}}\right), \tag{37}$$

which was first realized by Einwohner and Alder.[62] This expression provides an alternate method to the kinetic energy formula to compute the temperature from a MD simulation of a discrete potential system. This should be compared to the expressions for the configurational temperature[64–66] for continuous potential systems.

VI. EQUATION OF STATE

The pressure p of a pairwise additive system can be determined from the virial theorem

$$\frac{\beta p}{\rho} = 1 + \frac{\beta}{6N}\left\langle \sum_{jk} \mathbf{r}_{jk} \cdot \mathbf{F}_{jk} \right\rangle, \tag{38}$$

where N is the total number of atoms in the system, ρ is the number density of atoms, $\mathbf{r}_{jk}=\mathbf{r}_j-\mathbf{r}_k$, and $\mathbf{F}_{jk}$ is the force on atom j due to atom k.

For a discrete potential system (e.g., square-well or square-shoulder systems), the virial expression for the compressibility factor can also be written in terms of the event rates

$$\frac{\beta p}{\rho} = 1 + \frac{\beta}{3N\tau}\sum_{\text{event}} [\mathbf{r}_{ij} \cdot m_\alpha \Delta\mathbf{v}_i]_{\text{event}}, \tag{39}$$

where τ is the total elapsed time of the simulation. The summation is over all events that occur in the system and i and j are the atoms involved in the event. In event-driven molecular dynamics simulations, the pressure is typically calculated by accumulating the value of $\mathbf{r}_{ij}\cdot m_\alpha\Delta\mathbf{v}_i$ for each event in the system and using the above formula.

This expression can be simplified by dividing the events in the system into their different types and between the different pairs of species of atoms.

$$\begin{aligned}\frac{\beta p}{\rho} = 1 + \frac{\beta}{3N\tau}\sum_{\alpha,\alpha'} [&\mathcal{N}^{(1)}_{\alpha\alpha'}\langle \mathbf{r}_{ij} \cdot m_\alpha \Delta\mathbf{v}_i\rangle^{(1)} + \mathcal{N}^{(2)}_{\alpha\alpha'} \\ &\times \langle \mathbf{r}_{ij} \cdot m_\alpha \Delta\mathbf{v}_i\rangle^{(2)} + \mathcal{N}^{(3)}_{\alpha\alpha'}\langle \mathbf{r}_{ij} \cdot m_\alpha \Delta\mathbf{v}_i\rangle^{(3)} + \mathcal{N}^{(4)}_{\alpha\alpha'} \\ &\times \langle \mathbf{r}_{ij} \cdot m_\alpha \Delta\mathbf{v}_i\rangle^{(4)}],\end{aligned} \tag{40}$$

where $\mathcal{N}^{(k)}_{\alpha\alpha'}$ is the total number of events of type k between atoms of type α and α' in the system during the time τ. The brackets $\langle\cdots\rangle^{(k)}$ represent the average over events of type k. The term $\langle \mathbf{r}_{ij}\cdot m_\alpha\Delta\mathbf{v}_i\rangle^{(k)}$ is the mean contribution to the virial of an event of type k. If these were known, then Eq. (40) would directly relate the pressure of a system to the event rates between its atoms. In Sec. VI A, we develop an expression for each of these terms. Then these are used to develop an expression for the pressure in terms of only the event rates.

A. Mean contribution of an event to the virial

The mean contribution to the virial by an event of type k can be determined by averaging the momentum change of an atom over the on-event distribution of the collision diameter

$$\langle \mathbf{r}_{ij} \cdot m_\alpha \Delta\mathbf{v}_i\rangle^{(k)} = \int_{b^{(k)}_{ij,\min}}^{b^{(k)}_{ij,\max}} db_{ij}(\mathbf{r}_{ij} \cdot m_\alpha \Delta\mathbf{v}_i) f^{(k)}(b_{ij}).$$

On a core event, we find

$$\langle \mathbf{r}_{ij} \cdot m_\alpha \Delta\mathbf{v}_i\rangle^{(1)} = 2\mu_{\alpha\alpha'}\left(\frac{\pi\sigma^2}{2\beta\mu_{\alpha\alpha'}}\right)^{1/2}.$$

Core events give a positive contribution to the virial, increasing the pressure of the system above that of an ideal gas.

The average contribution to the virial due a capture event is

$$\begin{aligned}\langle \mathbf{r}_{ij} \cdot m_\alpha \Delta\mathbf{v}_i\rangle^{(2)} = \lambda\mu_{\alpha\alpha'}&\left(\frac{\pi\sigma^2}{2\beta\mu_{\alpha\alpha'}}\right)^{1/2} \\ &\times [1 - e^{\beta\varepsilon_{\alpha\alpha'}}Q(3/2,\beta\varepsilon_{\alpha\alpha'})],\end{aligned} \tag{41}$$

where $Q(n,x)$ is the incomplete Gamma function, defined as

$$Q(n,x) = \frac{1}{\Gamma(n)}\int_x^\infty dt t^{n-1}e^{-t},$$

and $\Gamma(n)$ is the Gamma function.[67] This contribution is always negative and will, therefore, tend to lower the pressure of the system. The average change of the virial due to a disassociation event is precisely the same as that of a capture event and, therefore, also tends to lower the pressure of the system. For the square-shoulder potential, the mean contribution of the release (type 2+) and association (type 3+) events to the virial is the negative of the contribution of the capture (type 2) events, and therefore, both tend to increase the pressure of the system.

The mean contribution to the virial due to a bounce event is

$$\begin{aligned}\langle \mathbf{r}_{ij} \cdot m_\alpha \Delta\mathbf{v}_i\rangle^{(4)} = -\frac{2\lambda\mu_{\alpha\alpha'}}{1 - e^{-\beta\varepsilon_{\alpha\alpha'}}}&\left(\frac{\pi\sigma^2}{2\beta\mu_{\alpha\alpha'}}\right)^{1/2} \\ &\times [1 - Q(3/2,\beta\varepsilon_{\alpha\alpha'})].\end{aligned} \tag{42}$$

This also has a negative contribution to the virial. For the square-shoulder potential, the bounce contribution has the opposite sign to the bounce contribution for the square-well potential and is always positive.

The variation of the contribution to the virial with temperature from each of the types of events is shown in Fig. 7 for a single component system of square-well atoms. In order to test the formulas for the contribution of each type of event to the virial, NVT molecular dynamics simulations were performed for single component square-well systems over a range of temperatures, densities, and well widths. The sym-

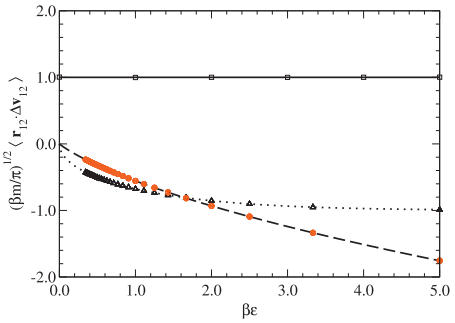

FIG. 7. Mean contribution to the virial of a pair of atoms on a (i) core event (solid line), (ii) capture or disassociation event (dashed line), and (iii) bounce event (dotted line) in a single component square-well system. The symbols are results from NVT MD simulations.

bols are the simulation results and the lines are the predictions. Excellent agreement is found between the two.

B. Event rate expression for the equation of state

Substituting the expressions for the mean contribution to the virial due to each type of event, developed in Sec. VI A, into Eq. (40) gives

$$\frac{\beta p}{\rho} = 1 + \sum_{\alpha\alpha'} \frac{(2\pi\beta\mu_{\alpha\alpha'}\sigma_{\alpha\alpha'}^2)^{1/2}}{3N\tau}[\mathcal{N}_{\alpha\alpha'}^{(1)} - \lambda_{\alpha\alpha'}\mathcal{N}_{\alpha\alpha'}^{(4)}]. \quad (43)$$

The contribution of the capture and disassociation events precisely cancel each other. Consequently, the pressure of a system of square-well atoms can be determined directly from the rates of only the core and bounce events. Specializing to the case of one-component systems of square-well atoms of diameter σ interacting with a square-well attractive potential of width λ and depth ε, this simplifies to

$$\frac{\beta p}{\rho} = 1 + \frac{(\pi\beta m\sigma^2)^{1/2}}{3N\tau}[\mathcal{N}^{(1)} - \lambda\mathcal{N}^{(4)}].$$

For square-shoulder systems, the corresponding formula is

$$\frac{\beta p}{\rho} = 1 + \sum_{\alpha\alpha'} \frac{(2\pi\beta\mu_{\alpha\alpha'}\sigma_{\alpha\alpha'}^2)^{1/2}}{3N\tau}[\mathcal{N}_{\alpha\alpha'}^{(1)} + \lambda_{\alpha\alpha'}\mathcal{N}_{\alpha\alpha'}^{(4+)}].$$

In the general case of a system of atoms interacting though a stepped potential, the pressure would be a sum of all the bounce rates of each of the steps of the potential multiplied by the distance of interaction. Steps which decrease with increasing atom separation would give a positive contribution, while steps which increase with increasing atom separation would give a negative contribution.

An alternate manner to derive the collision rate expression is to use the virial equation written in terms of the pair correlation function

$$\frac{\beta p}{\rho} = 1 + \frac{2\pi\rho}{3}\sum_{\alpha\alpha'} x_\alpha x_{\alpha'}\{\sigma_{\alpha\alpha'}^3 g_{\alpha\alpha'}(\sigma_{\alpha\alpha'}^+) + \sigma_{\alpha\alpha'}^3\lambda_{\alpha\alpha'}^3[g_{\alpha\alpha'}(\lambda_{\alpha\alpha'}\sigma_{\alpha\alpha'}^-) - g_{\alpha\alpha'}(\lambda_{\alpha\alpha'}\sigma_{\alpha\alpha'}^+)]\}. \quad (44)$$

Then, by using the relationships between the pair correlation functions and the event rates (see Sec. V), the event rate expression for the pressure can be obtained.

VII. CONCLUSIONS

The dynamics of systems composed of atoms interacting through stepped potentials, including square-well and square-shoulder systems, is driven by a series of events between pairs of atoms. These events can be divided into four types: core, capture/release, disassociation/association, and bounce. We have presented an analysis of the velocity statistics of atoms when they undergo each of these types of events. In particular, expressions were developed for the velocity distribution of a pair of atoms on an event.

Using this velocity distribution, the analytical expressions for the distribution of the kinetic energy and speed of an atom on an event were developed. In general, these differ from the Maxwell–Boltzmann distribution because atoms of differing speeds will undergo events at different rates. These expressions were validated against molecular dynamics simulation data. The pair correlation functions were related to the various event rates. From this it was found that the temperature of the system can be determined from the ratio of the rate of disassociation and bounce events. Finally, the mean contribution to the virial of each type of event was determined and this was used to construct an event rate formula for the pressure, which is only a function of the rate of core and bounce events.

For a hard sphere system, the pressure is determined solely by the collision rate. In a single component square-well system, there are two independent event rates: the core and bounce rates. The pressure was related to these event rates; however, the question arises as to whether a thermal property, such as the internal energy or the heat capacity, could be directly determined from the event rates. Can the thermodynamic properties of a discrete potential system be determined from knowledge of only the event rates?

One of the underlying assumptions of this work is that the system was large enough such that the velocities of the atoms could be considered independent and distributed according to the Maxwell–Boltzmann distribution. For small systems, the velocity distribution is not exactly given by the Maxwell–Boltzmann distribution.[68] We plan to examine the velocity and event statistics in these small systems in future.

ACKNOWLEDGMENTS

M.N. Bannerman acknowledges support from the EPSRC (U.K.) for the award of a Research Studentship. We are grateful to Professor David Corti for helpful discussions and comments.

APPENDIX: INVERSION OF THE LAPLACE TRANSFORMATIONS

In this section, we derive the expressions for the inverse Laplace transformations that are required for the kinetic energy distributions discussed in Sec. IV.

$$\tilde{f}(s) = \int_0^\infty \mathrm{d}t e^{-st} f(t). \tag{A1}$$

We first consider the function

$$\tilde{h}_1(s) = (s+1)^{-1}(s+a)^{-1/2}. \tag{A2}$$

Given the fact that the inverse Laplace transform of $s^{-1}(s+a)^{-1/2}$ is $a^{-1/2}\,\mathrm{erf}(\sqrt{at})$ (see Ref. 69) and using the relation

$$\tilde{f}(s+a) \leftrightarrow e^{-at} f(t), \tag{A3}$$

we can derive

$$h_1(t;a) = (a-1)^{-1/2}\mathrm{erf}(\sqrt{(a-1)t})e^{-t}. \tag{A4}$$

Next, we examine the function

$$\tilde{h}_0(s;a) = \frac{(s+a)^{1/2}}{(s+1)^2}.$$

This can be split into two terms

$$\tilde{h}_0(s;a) = (s+1)^{-1}(s+a)^{-1/2} + (a-1)(s+1)^{-2}(s+a)^{-1/2}.$$

With the knowledge of the inverse Laplace transform of $s^{-1}(s+a)^{-1/2}$ and using Eq. (A3) and the relation

$$s^{-1}\tilde{f}(s) \leftrightarrow \int_0^t \mathrm{d}\tau f(\tau),$$

we find

$$h_0(t;a) = t^{1/2}\left[\frac{e^{-(a-1)t}}{\pi^{1/2}} + \frac{1+2(a-1)t}{2\sqrt{(a-1)t}}\mathrm{erf}(\sqrt{(a-1)t})\right]e^{-t}.$$

Finally, we consider the function

$$\tilde{f}(s) = \frac{(s+a)^{1/2}}{(s+1)^2}\exp\left[-w\left(\frac{s+1}{s+a}\right)\right],$$

which is required in the kinetic energy distribution for the disassociation and bounce events (see Sec. IV). The exponential can be expressed in terms of a power series in the variable w, which can be grouped into three main terms

$$\tilde{f}(s) = \sum_{n=0}^\infty \frac{(s+1)^{n-2}}{(s+a)^{n-1/2}}\frac{(-w)^n}{\Gamma(n+1)} = \tilde{h}_0(s;a) - w\tilde{h}_1(s;a) + \tilde{h}_2(s;a,w),$$

where

$$\tilde{h}_2(s;a,w) = \sum_{n=0}^\infty \frac{(s+1)^n}{(s+a)^{n+3/2}}\frac{(-w)^{n+2}}{\Gamma(n+3)}.$$

By using the fact that the inverse Laplace transform of s^{-k} is $t^{k-1}/\Gamma(k)$ and the relation[69]

$$s^n\tilde{f}(s) - s^{n-1}f(0) - s^{n-2}\frac{\mathrm{d}f(0)}{\mathrm{d}t} - \cdots s\frac{\mathrm{d}^{n-2}f(0)}{\mathrm{d}t^{n-2}} - \frac{\mathrm{d}^{n-1}f(0)}{\mathrm{d}t^{n-1}} \leftrightarrow \frac{\mathrm{d}^n f(t)}{\mathrm{d}t^n}, \tag{A5}$$

we find that the inverse Laplace transform of $(s+1)^n/(s+a)^{n+3/2}$ is

$$\frac{\mathrm{d}^n}{\mathrm{d}t^n}(t^{n+1/2}e^{-(a-1)t}) = a^{-1/2}\Gamma(n+1)t^{1/2}e^{-at}L_n^{1/2}((a-1)t),$$

where L_n^k is an associated Laguerre polynomial.[67] Substituting this, we find

$$\begin{aligned} h_2(t;a,w) &= t^{1/2}e^{-at}\sum_{n=0}^\infty \frac{L_n^{1/2}((a-1)t)}{\Gamma(n+1/2+1)}\frac{(-w)^{n+2}}{(n+2)(n+1)} \\ &= \sqrt{\frac{t}{\pi}}e^{-at}\left\{\left[\sqrt{\frac{w}{(a-1)t}}\sinh(2\sqrt{w(a-1)t}) + \cosh(2\sqrt{w(a-1)t})\right]e^{-w} - 1\right\} \\ &\quad - \frac{e^{-t}}{4\sqrt{a-1}}(-1+2w-2(a-1)t) \\ &\quad \times [\mathrm{erf}(\sqrt{(a-1)t} - \sqrt{w}) + \mathrm{erf}(\sqrt{(a-1)t} + \sqrt{w}) \\ &\quad - 2\,\mathrm{erf}(\sqrt{(a-1)t})]. \end{aligned} \tag{A6}$$

The summation was written in closed form by twice integrating the following identity:[70]

$$\sum_{n=0}^\infty \frac{L_n^k(x)}{\Gamma(n+k+1)}(-w)^n = e^w(xw)^{-k/2}I_k(2\sqrt{xw}),$$

where I_k is a modified Bessel function of the first kind, with respect to w.

[1] D. Henderson, J. A. Barker, and W. R. Smith, J. Chem. Phys. **64**, 4244 (1976).
[2] S. B. Yuste and A. Santos, J. Chem. Phys. **101**, 2355 (1994).
[3] A. Lang, G. Kahl, C. N. Likos, H. Löwen, and M. Watzlawek, J. Phys.: Condens. Matter **11**, 10143 (1999).
[4] J. Largo, J. R. Solana, S. B. Yuste, and A. Santos, J. Chem. Phys. **122**, 084510 (2005).
[5] M. A. Glaser, G. M. Grason, R. D. Kamien, A. Košmrlj, C. D. Santangelo, and P. Ziherl, EPL **78**, 46004 (2007).
[6] S. Hlushak, A. Trokhymchuk, and S. Sokołowski, J. Chem. Phys. **130**, 234511 (2009).
[7] B. J. Alder, D. A. Young, and M. A. Mark, J. Chem. Phys. **56**, 3013 (1972).
[8] D. Henderson, W. G. Madden, and D. D. Fitts, J. Chem. Phys. **64**, 5026 (1976).
[9] D. M. Heyes, J. Chem. Soc., Faraday Trans. **87**, 3373 (1991).
[10] D. M. Heyes and P. J. Aston, J. Chem. Phys. **97**, 5738 (1992).
[11] S. Labik, A. Malijevsky, R. Kao, W. R. Smith, and R. D. Rio, Mol. Phys. **96**, 849 (1999).
[12] S. B. Kiselev, J. F. Ely, L. Lue, and J. R. Elliott, Fluid Phase Equilib. **200**, 121 (2002).
[13] J. Largo, J. R. Solana, L. Acedo, and A. Santos, Mol. Phys. **101**, 2981 (2003).
[14] M. J. Uline and D. S. Corti, J. Chem. Phys. **129**, 014107 (2008).
[15] L. Vega, E. de Miguel, L. F. Rull, G. Jackson, and I. A. McLure, J. Chem. Phys. **96**, 2296 (1992).
[16] G. Orkoulas and A. Z. Panagiotopoulos, J. Chem. Phys. **110**, 1581 (1999).

[17] F. Del Rio, E. Avalos, R. Espindola, L. F. Rull, G. Jackson, and S. Lago, Mol. Phys. **100**, 2531 (2002).
[18] E. de Miguel, Phys. Rev. E **55**, 1347 (1997).
[19] J. R. Elliott and L. Hu, J. Chem. Phys. **110**, 3043 (1999).
[20] D. L. Pagan and J. D. Gunton, J. Chem. Phys. **122**, 184515 (2005).
[21] R. López-Rendón, Y. Reyes, and P. Orea, J. Chem. Phys. **125**, 084508 (2006).
[22] H. L. Vörtler, K. Schäfer, and W. R. Smith, J. Phys. Chem. B **112**, 4656 (2008).
[23] J. K. Singh, D. A. Kofke, and J. R. Errington, J. Chem. Phys. **119**, 3405 (2003).
[24] P. Orea, Y. Duda, and J. Alejandre, J. Chem. Phys. **118**, 5635 (2003).
[25] P. Orea, Y. Duda, V. C. Weiss, W. Schroer, and J. Alejandre, J. Chem. Phys. **120**, 11754 (2004).
[26] G. J. Gloor, G. Jackson, F. J. Blas, and E. de Miguel, J. Chem. Phys. **123**, 134703 (2005).
[27] E. de Miguel, J. Phys. Chem. B **112**, 4674 (2008).
[28] D. A. Young and B. J. Alder, J. Chem. Phys. **73**, 2430 (1980).
[29] A. Lomakin, N. Asherie, and G. B. Benedek, J. Chem. Phys. **104**, 1646 (1996).
[30] H. Liu, S. Garde, and S. Kumar, J. Chem. Phys. **123**, 174505 (2005).
[31] S. B. Kiselev, J. F. Ely, and J. J. R. Elliott, Mol. Phys. **104**, 2545 (2006).
[32] C. Rascón, E. Velasco, L. Mederos, and G. Navascués, J. Chem. Phys. **106**, 6689 (1997).
[33] J. Serrano-Illán, G. Navascués, and E. Velasco, Phys. Rev. E **73**, 011110 (2006).
[34] B. J. Alder and T. E. Wainwright, Phys. Rev. A **1**, 18 (1970).
[35] W. E. Alley and B. J. Alder, J. Chem. Phys. **63**, 3764 (1975).
[36] J. P. J. Michels and N. J. Trappeniers, Chem. Phys. Lett. **66**, 20 (1979).
[37] J. P. J. Michels and N. J. Trappeniers, Physica A **101**, 156 (1980).
[38] J. P. J. Michels and N. J. Trappeniers, Physica A **104**, 243 (1980).
[39] J. P. J. Michels and N. J. Trappeniers, Physica A **107**, 158 (1981).
[40] J. P. J. Michels and N. J. Trappeniers, Physica A **107**, 299 (1981).
[41] J. P. J. Michels and N. J. Trappeniers, Physica A **116**, 516 (1982).
[42] H. Wilbertz, J. Michels, H. van Beijeren, and J. A. Leegwater, J. Stat. Phys. **53**, 1155 (1988).
[43] C. G. Joslin, C. G. Gray, J. P. J. Michels, and J. Karkheck, Mol. Phys. **69**, 535 (1990).
[44] H. Sigurgeirsson and D. M. Heyes, Mol. Phys. **101**, 469 (2003).
[45] D. C. Rapaport, J. Chem. Phys. **71**, 3299 (1979).
[46] S. W. Smith, C. K. Hall, and B. D. Freeman, J. Comput. Phys. **134**, 16 (1997).
[47] Y. Zhou, C. Hall, and M. Karplus, Phys. Rev. Lett. **77**, 2822 (1996).
[48] Y. Zhou, M. Karplus, J. Wichert, and C. Hall, J. Chem. Phys. **107**, 10691 (1997).
[49] J. E. Magee, V. R. Vasquez, and L. Lue, Phys. Rev. Lett. **96**, 207802 (2006).
[50] M. N. Bannerman, J. E. Magee, and L. Lue, Phys. Rev. E **80**, 021801 (2009).
[51] A. V. Smith and C. K. Hall, J. Chem. Phys. **113**, 9331 (2000).
[52] A. V. Smith and C. K. Hall, J. Mol. Biol. **312**, 187 (2001).
[53] J. E. Magee, J. Warwicker, and L. Lue, J. Chem. Phys. **120**, 11285 (2004).
[54] H. D. Nguyen and C. K. Hall, Biophys. J. **87**, 4122 (2004).
[55] H. D. Nguyen and C. K. Hall, J. Am. Chem. Soc. **128**, 1890 (2006).
[56] G. Chapela, L. E. Scriven, and H. T. Davis, J. Chem. Phys. **91**, 4307 (1989).
[57] R. van Zon and J. Schofield, J. Chem. Phys. **128**, 154119 (2008).
[58] J. R. Elliott, Fluid Phase Equilib. **194–197**, 161 (2002).
[59] O. Unlu, N. H. Gray, Z. N. Gerek, and J. R. Elliott, Ind. Eng. Chem. Res. **43**, 1788 (2004).
[60] L. Lue, J. Chem. Phys. **122**, 044513 (2005).
[61] B. J. Alder and T. E. Wainwright, J. Chem. Phys. **31**, 459 (1959).
[62] T. Einwohner and B. J. Alder, J. Chem. Phys. **49**, 1458 (1968).
[63] J. A. Barker and D. Henderson, Rev. Mod. Phys. **48**, 587 (1976).
[64] H. H. Rugh, Phys. Rev. Lett. **78**, 772 (1997).
[65] B. D. Butler, G. Ayton, O. G. Jepps, and D. J. Evans, J. Chem. Phys. **109**, 6519 (1998).
[66] G. Rickayzen and D. M. Heyes, J. Chem. Phys. **127**, 144512 (2007).
[67] G. Arfken, *Mathematical Methods for Physicists*, 3rd ed. (Academic, San Diego, 1985).
[68] M. J. Uline, D. W. Siderius, and D. S. Corti, J. Chem. Phys. **128**, 124301 (2008).
[69] M. R. Spiegel, *Laplace Transforms* (McGraw-Hill, New York, 1965).
[70] G. Szegö, *Orthogonal Polynomials*, 4th ed. (American Mathematical Society, Providence, 1975).